Report Rapport

INFO 0356

Atomic Energy Control Board
Commission de contrôle de l'énergie atomique

GAS AND WATER PERMEABILITY TESTS OF 25 YEAR OLD CONCRETE FROM THE NPD NUCLEAR GENERATING STATION

by

R.H. Mills
University of Toronto

Canada

INFO-0356

Atomic Energy Control Board
P.O. Box 1046
Ottawa, Canada
K1P 5S9

Commission de contrôle de l'énergie atomique
C.P. 1046
Ottawa, Canada
K1P 5S9

GAS AND WATER PERMEABILITY TESTS OF 25 YEAR OLD CONCRETE FROM THE NPD NUCLEAR GENERATING STATION

by

R.H. Mills
University of Toronto

A research report prepared for the
Atomic Energy Control Board
Ottawa, Ontario

Project No. 2.147.1

May 1990

Canada

Research report

GAS AND WATER PERMEABILITY OF 25 YEAR OLD CONCRETE FROM THE NPD NUCLEAR GENERATING STATION

ABSTRACT

Permeability tests on cores recovered from concrete which had been in service for 25 years in the Nuclear Power Demonstration (NPD) reactor showed rates of mass transfer of gas and water which were greater than young fresh concrete of the same proportions and that previously reported in AECB reports 0011, 0188-1 and 0188-2. This "transparency" of the concrete was also 2 orders of magnitude greater than that of comparable concrete which had been stored in the laboratory atmosphere for 19 years.

Analysis of the effluent in water permeability tests revealed the presence of unusual amounts of soluble materials, mainly Na and K but little Ca, in the reactor concrete. This suggested service-related deterioration of the concrete rather than the release of soluble Ca by continuing hydration of cement.

RÉSUMÉ

Les épreuves de perméabilité auzquelles ont été soumises des carottes prises à même le béton en place dans le réacteur NPD (Nuclear Power Demonstration) depuis 25 ans ont indiqué des débits de transfert de masse de gaz et d'eau supérieurs à ceux du béton jeune et frais de mêmes proportions, qui avaient été rapportés dans les rapports INFO-0111, INFO-0188-1 et INFO-0188-2 de la CCEA. La "transparence" du béton était aussi plus grande par deux ordres de grandeur que le béton comparable qui avait été entreposé dans l'atmosphère du laboratoire durant 19 ans.

L'analyse de l'effluent après les épreuves de perméabilité en eau a révélé la présence de quantités inhabituelles de matières solubles, surtout du sodium et du potassium, mais peu de calcium, dans le béton du réacteur. Ceci laisse supposer que la détérioration du béton est due à des réparations plutôt qu'au rejet de calcium soluble par hydratation continue du ciment.

GAS AND WATER PERMEABILITY OF 25 YEAR OLD CONCRETE FROM THE NPD NUCLEAR GENERATING STATION

SUMMARY

The de-commissioning of Canada's first nuclear power plant, the Nuclear Power Demonstration (NPD), afforded an opportunity to assess aging effects on concrete which had been exposed to high temperature and high radiation in a typical service environment.

Horizontal concrete cores recovered from key locations, including walls separating low and high exposure zones, were subjected to gas and water permeability tests on specimens taken from both ends and the middle of the core.

The results indicate increased "transparency" to both water and gas in the NPD cores compared with those reported for freshly poured concrete (AECB Report INFO-0188), the ratios varying between 5 and 30 for water and between 150 and 500 for gas.

When the results of permeability tests on specimens with visible defects were neglected, the permeabilities, expressed as a factor times the permeability of control specimens, ranged from 50 to 362. Expressed as annual mass transfer through 1000 m^2 of 1 m thick concrete, the range was 44,100 kg to 321,500 kg. The corresponding value for the control specimens was 889 kg.

For the NPD concrete, water permeability tests were complicated by variation of the flow rate with time: the flow at 120 minutes varying from one quarter to one thirtieth of that determined at the beginning of the test (say at 4 minutes). This effect was also seen in comparable concrete which was stored in the laboratory atmosphere for 19 years.

Initially it was observed that the apparent reduction of permeability was accompanied by loss of weight of the specimen. At the same time, analysis of the effluent showed dissolved solids, typically Ca^{++}, K^+ and Na^+, amounting to between 1860 and 6132 mg/l (ppm) for the NPD concrete and 385 ppm for the control concrete.

That the reduction of permeability was due to further hydration of cement during the course of the test therefore appeared unlikely. Instead it may be postulated that flow of water through the specimen sets up a gradient of dissolved solids, with concentration increasing towards the outlet. Supersaturation of the pore solution towards the outlet, would result in precipitation of solids in the pores, thus forming a filter-cake and increasing resistance to flow. In order to verify this model the direction of flow was reversed and, as expected, the flow rate was reset nearer to the original value. An alternative hypothesis envisions the blockage as being caused by loose solids being transported in the water stream and precipitated towards the outlet. This latter hypothesis is inconsistent with the appearance of the effluent which was clear solution.

There is a clear indication that NPD concrete contained more soluble material, mainly Na^+ and K^+, than the control concrete. It appeared that free lime was a minor constituent of the dissolved solids so that this phenomenon could not be ascribed to dissolved $Ca(OH)_2$

resulting from increased hydration of the 25 year old concrete. The difference could be associated with the use of slightly reactive aggregates in the NPD concrete. The highest solubility for site 4 (between the steam generator vault and the turbine hall) coincides with maximum exposure to high temperature, radiation and stress. The minimum value for site 11 (turbine block) coincides with moderate temperature and zero radiation.

A prime objective of the present work was to assess the effect of aging on the NPD concrete. As far as permeability is concerned, the degree of deterioration was unlikely to have rendered the concrete unserviceable during the 25 year life of the structure although this conclusion must be advanced with some caution due to the innate variability of the concrete and the test results.

The solubility of the NPD concrete warrants further investigation because it calls into question the long-term durability of concrete and because soluble Na^+ and K^+ has been associated with diminished bond strength between concrete and reinforcing steel.

The concept of a single parameter description of the mass transfer characteristics of concrete, say k or D^*, is flawed because this quantity is influenced by reaction between concrete and water during the test and is also dependent on pressure. It seems that design criteria and associated standards for dependable quality assurance have to be advanced beyond the simple D'Arcian model.

TABLE OF CONTENTS Page

TABLE OF CONTENTS cont'd

APPENDICES

LIST OF TABLES

LIST OF FIGURES

LIST OF SYMBOLS

A	cross-sectional area
C	cement content of concrete, kgm^{-3}
D*	gas permeability, m^2
D*	water permeability, m^2
V_{gel}	gel water
V_m	monolayer capacity of cement paste per unit mass of cement
W	water content of cement or concrete, kgm^{-3}
k	permeability coefficient, non-specific ($= D^*/\mu$)
w_e	mass ratio of evaporable water per unit of cement
w_n	mass ratio of non-evaporable water
w_o	mass ratio of total water per unit of cement
x	distance along flow path
α^*	ultimate mass fraction of hydrated cement
ρ	density
μ	fluid viscosity
Σ_{BET}	specific surface area of cement paste, as determined by BET method

1. INTRODUCTION

Under normal service conditions, aging of concrete results in changes of pore size distribution, micro-cracking due to shrinkage, and reduced alkalinity. In the service conditions of a nuclear power plant all of these changes may be accelerated by high temperature and excitation by radiation, and, in addition, factors as yet unknown, may be anticipated.

Previous work (Reports INFO-0111 and INFO-0188 published by the AECB) concluded that sound concrete was an effective barrier against the transport of gas and water but that construction defects or cracks arising from service conditions might result in significant impairment of this function.

Unstable compounds in cement such as C_3A* and CH* are likely to be affected by exposure to elevated temperatures combined with radiation. An important aspect of CH instability concerns the bond and passivation of reinforcing steel since there is a concentration of this material at the steel interface.

In order to simulate these aging effects in the laboratory some distortion in the natural relationship between temperature rise and the rate of radiation dosage would be required. For instance, if one applied the integrated radiation dosage over a short period of weeks, the accompanying thermal shock might destroy the concrete.

1.1 NPD Concrete

The recovery of concrete from the Nuclear Plant Demonstration (NPD) reactor offered a unique opportunity to study concrete manufactured under real site conditions and exposed to real service environments for some 25 years.

* Standard nomenclature: C_3A = Tri-calcium, aluminate, CH = Calcium Hydroxide.

Originally it was intended to "de-contaminate" the concrete at the laboratories of Ontario Hydro before delivery to the laboratory at the University of Toronto. In the event this was not possible (refer to Figure 2 for locations of cores):

> Cores 1 and 2 were highly radioactive and were retained in Ontario Hydro storage until appropriate handling could be arranged.
>
> Cores 3, 4 and 5 were accepted, although radioactive, but testing was delayed until handling facilities were built and approved by the University of Toronto Radiation Protection Office.
>
> Cores 9 and 11 were originally stated to be free of radioactive contaminants and testing was completed between April and August, 1988. In November, after testing of these cores was complete, Ontario Hydro issued a warning that Cores 9A and 9C contained tritium (the tritium concentration was extremely feeble to cause any health hazards to the laboratory personnel).

1.2 Perspective on the Permeability of Concrete

At the time of construction of the NPD reactor, commercially available concrete ranged from low strength (25 MPa), to high strength (50 MPa). The corresponding range in water permeability probably ranged from k = 15 to 2800 x 10 E - 12 m/s (1).

Test data available at that time from the United States Bureau of Reclamation gave values of k averaging 39 x 10 E - 12 m/s for field concrete having water/cement ratios varying from 0.46 to 0.86 (2).

Recent work (3) on concrete of various dimensions, driving pressure and confining pressure gave values ranging from k = 0.3 to 0.7 x 10 E - 12 m/s.

Table 1

Correlation of Permeability with Strength (Richard Berger 1989 (1))

Class	Strength	Range in k x 10 E - 12 m/s
Low Strength	25 MPa	300 - 2800*
Average Strength	35 MPa	700 - 2000
High Strength	50 MPa	15 - 70

* This means 2800 x 10^{-12} m/s

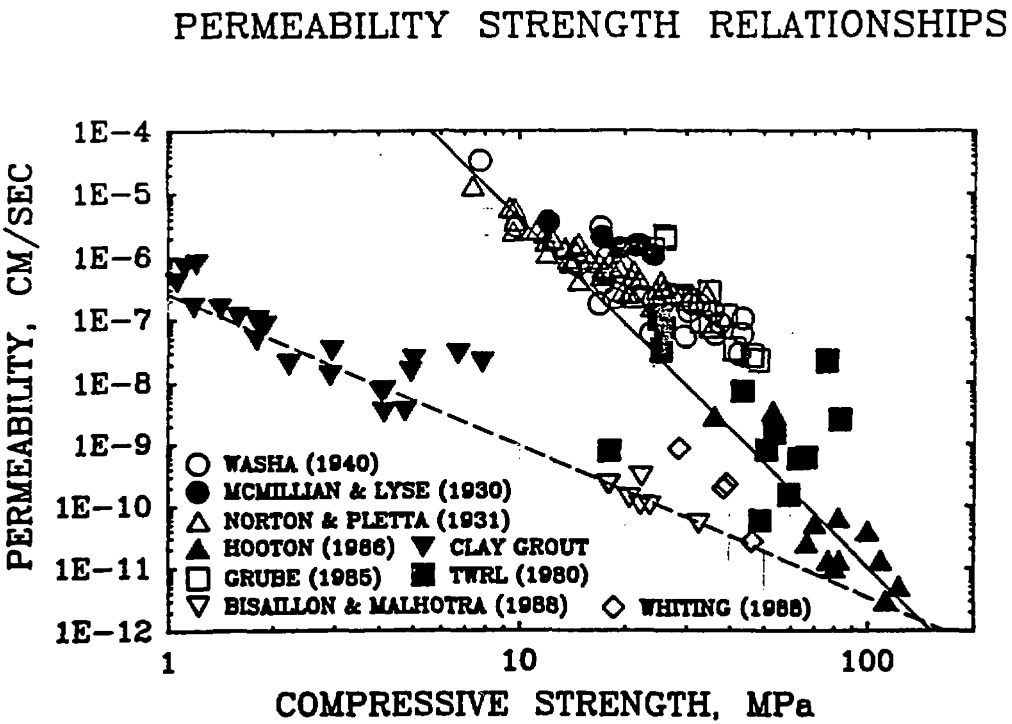

Fig. 1 Berger's proposed relationship between strength and permeability (1). The lower curve refers to clayey soils while the upper curve refers to concrete and cement pastes.

Table 2

Perspective on widely quoted data from Technical Memorandum No. 6-380 of the U.S. Waterways Experimental Station [Ref. 2].

	Report Mix Data			Calculated	
No. of Observations	Water:Cement ratio	Cement kgm^3	Water kg/m^3	Permeability $10^{-12}ms^{-1}$	S.D. $10^{-12}ms^{-1}$
5	0.6	223	134	48*	32*
2	0.86	112	96	84	27
3	0.65	140	91	49	17
5	0.69	156	108	8	10
5	0.75	140	105	34	12
5	0.74	153	113	24	5
4	0.58	168	97	41	50
1	0.46	223	103	27	-

* This means 48 x 10^{-12} m/s

In another investigation of the permeability of cement pastes containing a range of cement substitutes (4) the range in k values at 7 days was from 0.5 to 250 x 10 E - 12 m/s and at 91 days from k = 0.01 to 0.13 x 10 E - 12 m/s.

Taking account of a wide range of concrete quality, initial porosity and cement composition it thus appeared that the permeability of the NPD concrete should not exceed 2800 x 10 E - 12 m/s except for easily visible construction defects or structural cracks.

Table 3 [Hooton and Wakely (3)]

Average k Values, Concrete with 0% Fly Ash, 3-Way Analysis of Variance

Variable	Average k values (x 10^{-13} m/s)
Specimen length, in*	
4.5	6.9**
7.1	3.6
Driving pressure, psi*	
200	5.5
400	3.1
C/D ratio*	
2	3.6
4	3.0
6	7.1

* 4.5 and 7.1-in. specimens not separated.

** This means 6.9 x 10^{-13} m/s.

Table 4

Coefficient of Permeability of Pastes (Hooton (4))

Cementing Materials	w/s**	Coefficient of Permeability, 10^{-13} m/s 7 days	28 days	91 days	182 days
100% SRPC	0.25	6.3*	3.8	1.3	0.3
35% FA	0.25	5.1	1.3	0.5	<0.3
65% BFS	0.25	28.0	5.1	0.1	<0.1
10% SF	0.25	10.0	0.9	0.6	0.4
20% SF	0.25	6.3	<0.1	0.3	<0.1
100% SRPC	0.36	340.0	2.5	1.3	1.0
25% FA	0.36	140.0	2.5	0.5	0.3
35% FA	0.36	280.0	...	...	...
50% BFS	0.36	265.0	6.3	0.6	<0.3
65% BFS	0.36	2500.0	6.3	1.3	0.4

* This means 6.3 x 10^{-13} m/s

** w/s means the mass ratio of water to cementitious material

2. EXPERIMENTAL

2.1 Core Recovery and Preparation

Core drilling, 145 mm diameter, was undertaken by Ontario Hydro at the sites indicated in Fig. 2. Figures 3, 4 and 5 show drilling operation and grouping of cores. Fig. 6 illustrates one of the difficulties encountered when the drill strikes a reinforcing bar. It was not possible to drill a single continuous core from the structure and instead a number of pieces 240 mm to 400 mm in length were recovered. These were sealed in polythene bags and sent to the Ontario Hydro's Kipling research laboratory. After assessment of the level of radioactivity, the cores listed in Table 5 were sent to the University of Toronto.

Table 5

Location Service Environment and Characteristics of Cores

Core Reference	Location	Exposure * Temperature/Radiation/Stress	Density kg/m^3	Void Space per cent
3	Dump tank to soil	3/3/5 *	2383	14.6
4	Boiler room to condenser room	5/5/5	2385	14.1
5	Boiler room to soil	5/5/5	2364	14.3
9	Pressure relief duct to soil	1/1/5	2320	18.0
11	Turbine block	3/0/5	2401	13.7

* On a scale of 0 to 5, 3/3/5 means Medium Temperature, Medium Radiation, High Structural Stress.

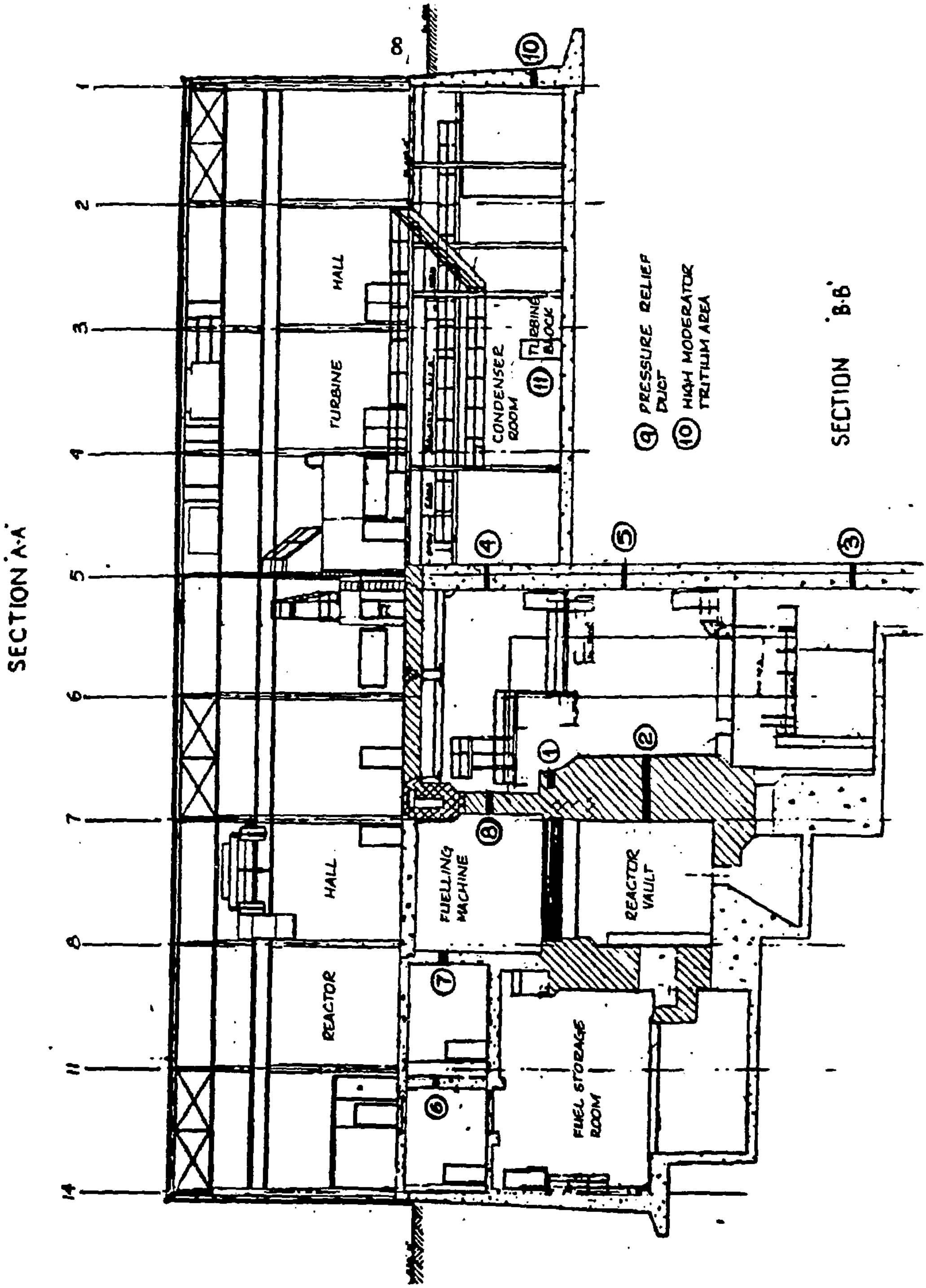

Fig. 2 Location of cores drilled by Ontario Hydro

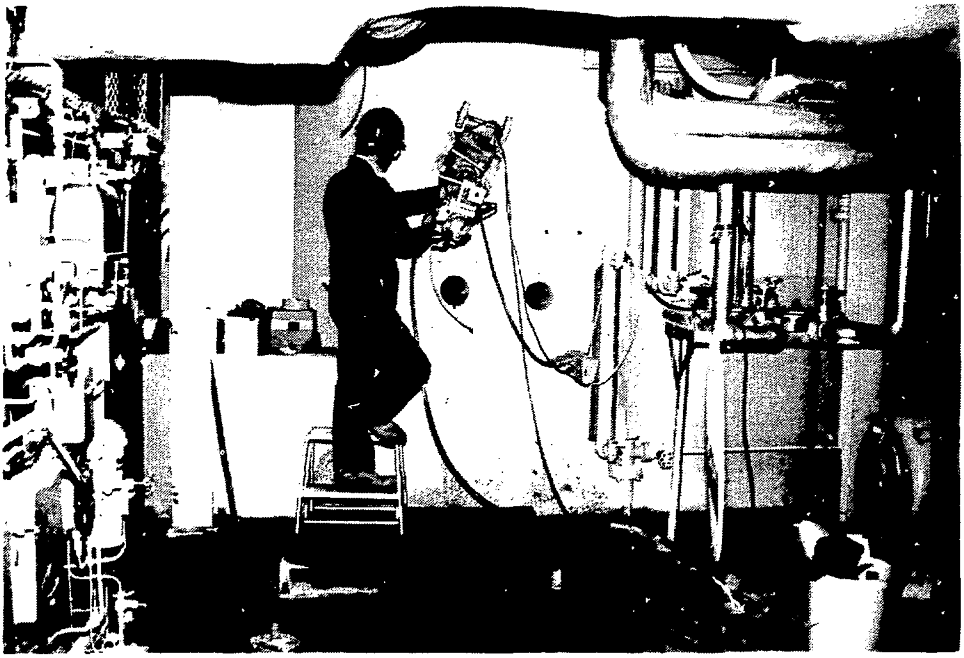

Fig. 3
Core Drilling
at location 11

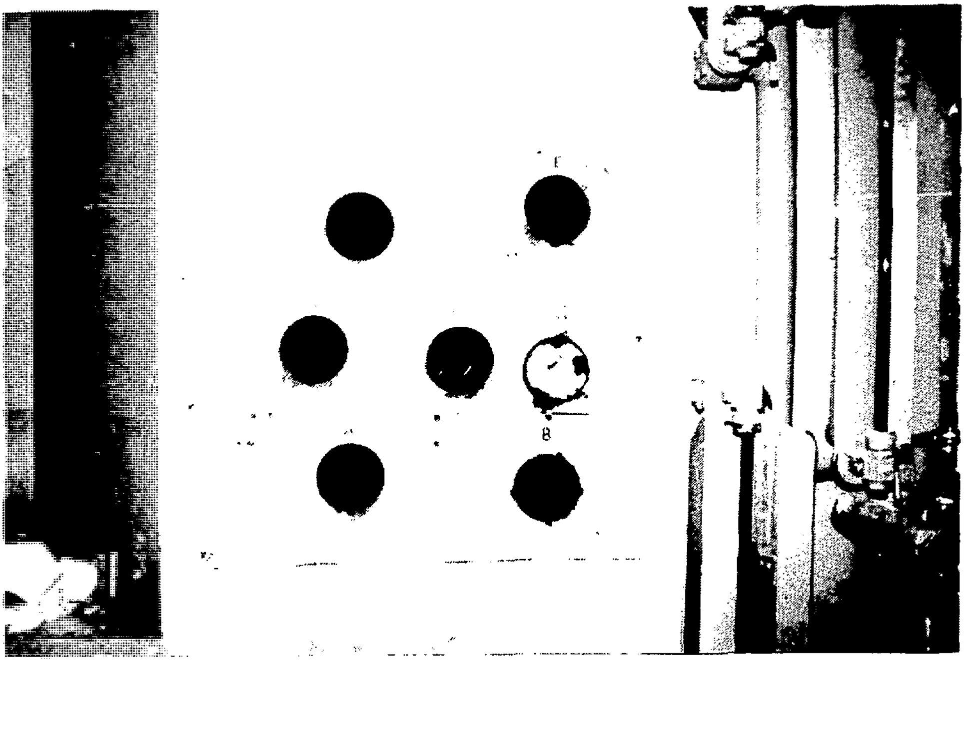

Fig. 4
Pattern of
Holes at site 11

Fig. 5

Core recovery from sites 3, 5 and 9

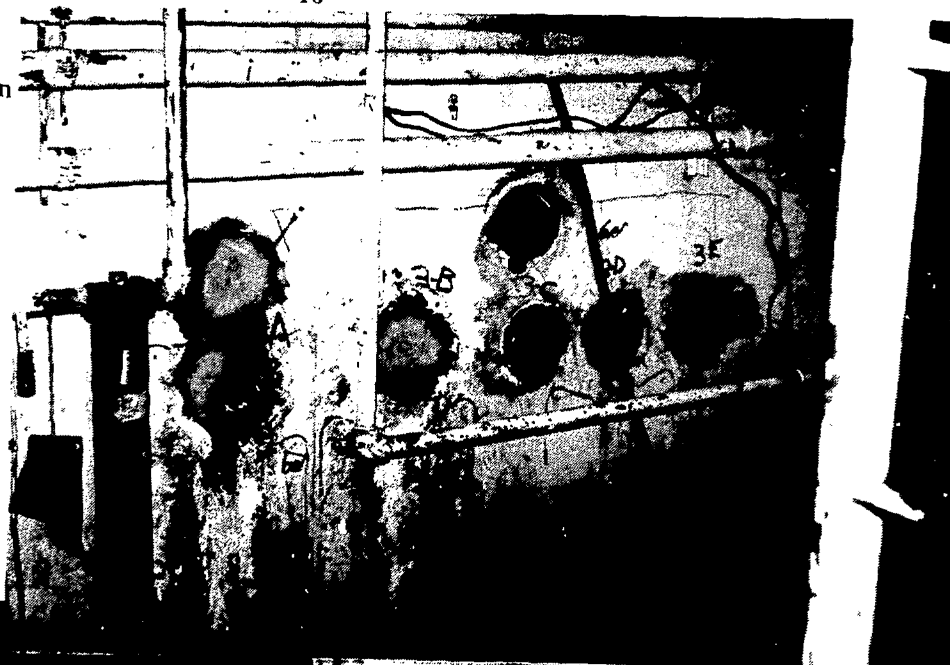

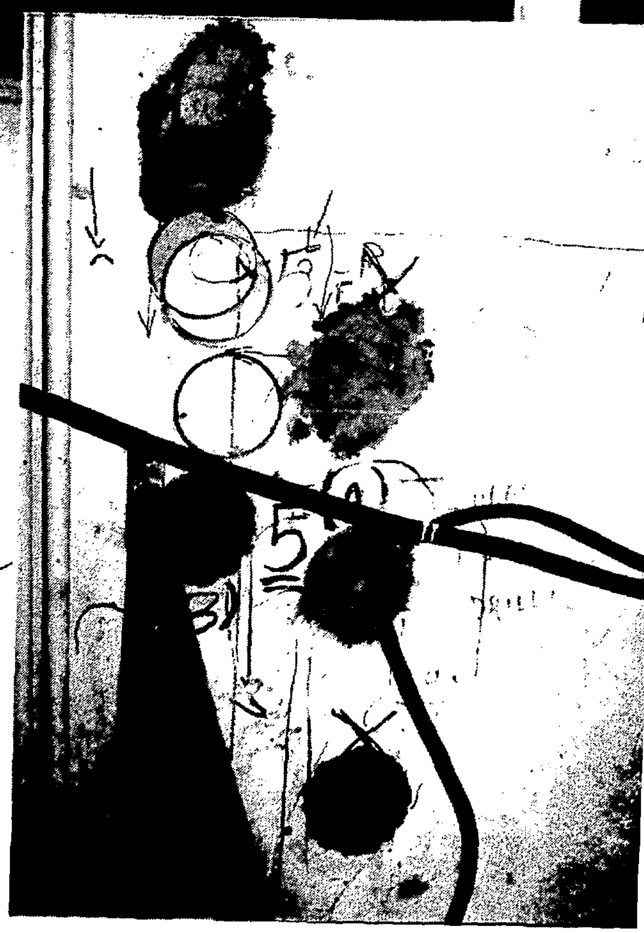

Fig. 6 Intersection of core drill with a reinforcing bar at site 4

Fig. 7 Cores 9 and 11 as they were received at the University of Toronto showing typical 200-400 mm long pieces of core.

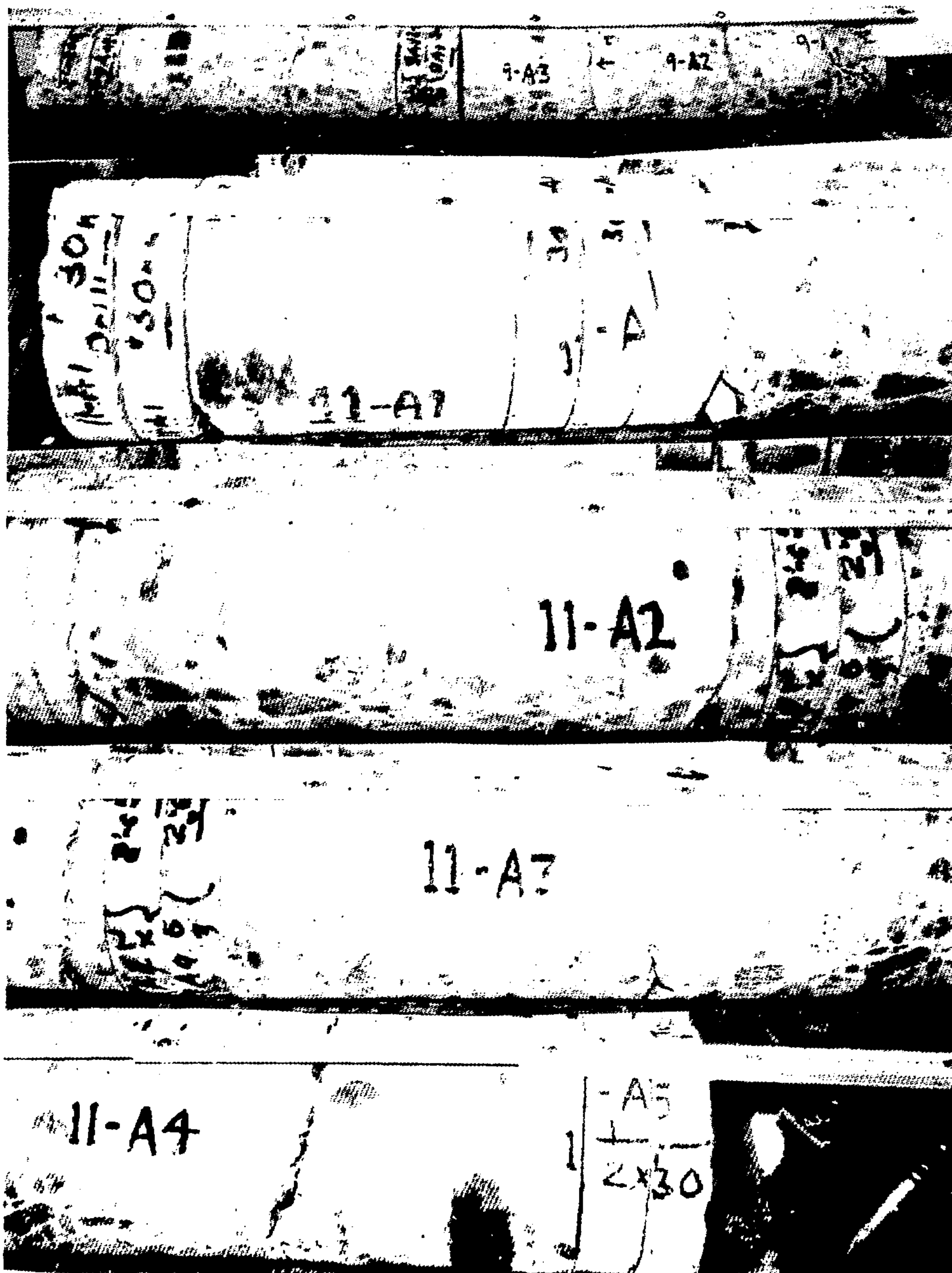

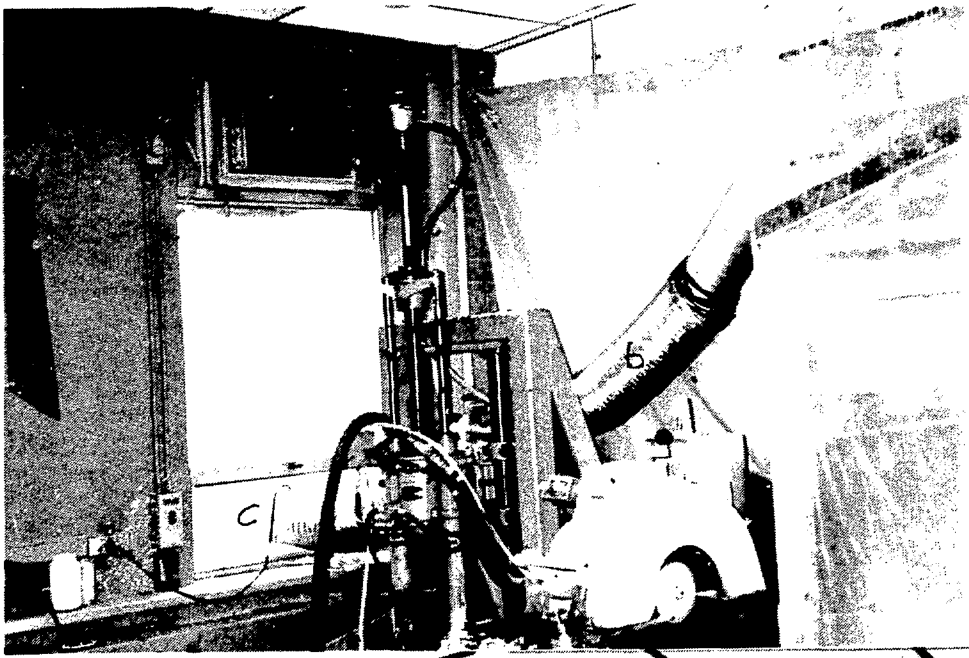

Fig. 8
Enclosure and exhaust for cutting radioactive specimens
(a) Polythene tent
(b) Duct
(c) Vent-axia exhaust fan

Fig. 9

Permeability Apparatus

A Gas-water cylinder with double-acting piston
B Gas manifold
C Concrete specimen
D Aluminium cylinder
E RTV rubber cylinder
F Water manifold
G Gas burette or micro-balance

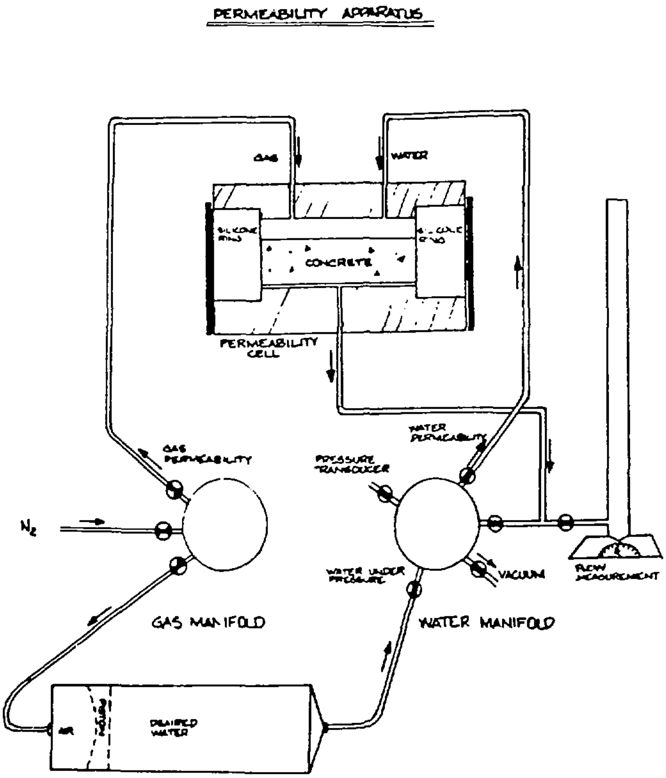

The cores were cut into discs, 32 mm thick, using a diamond saw which was enclosed in a polythene covered tent equipped with a filtered duct and fan exhausting to atmosphere as seen in Fig. 8.

Immediately after cutting, the cores were washed in running water and then conditioned in the laboratory atmosphere at approximately 60 per cent relative humidity.

2.2 Gas Permeability

The specimens were then placed in the permeameter (Figures 9 and 10) and exposed to 345 kPa over pressure of Nitrogen at the inlet. The volume of gas transferred was measured by means of a gas burette at the outlet. This was repeated for different moisture contents.

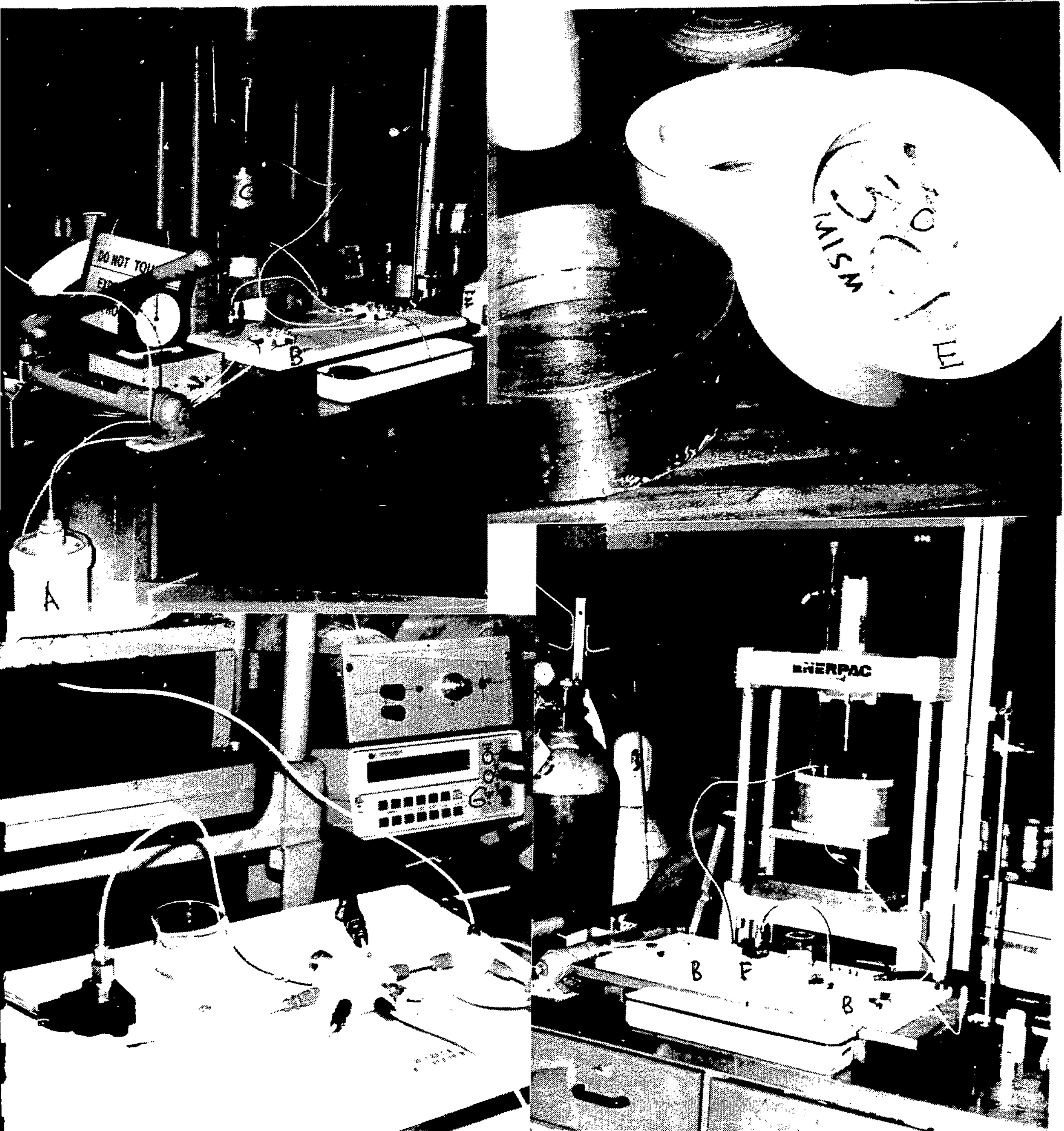

Fig. 10Permeability Apparatus: A Gas-water cylinder, B Gas manifold, C Concrete specimen, D Aluminium cylinder, E RTV rubber cylinder, F Pressure transducer, G Pressure read-out

2.3 Water Permeability

After the final gas diffusion test, at a moisture content designed to give about 10 volume per cent of free space, the cores were vacuum saturated and water permeability was determined on the same apparatus (Figs. 9 and 10).

2.4 Oven-dry state

Following the water permeability tests the specimens were dried to constant weight at 110°C. Total porosity ϵ was determined from the corresponding moisture loss from the saturated, surface-dry state. A final (maximum) value for gas diffusion was determined in the oven-dry state.

2.5 Control concrete

Original mix proportions were estimated from the densities and porosities of cores taken from Site 11 using the model given in Appendix A of Report INFO-0188 and in Appendix B of this report. The mix proportions are given in Table 6.

Table 6
Proportions of control mix kg/m^3

	Mass kg	Volume m^3
Cement	303.4	0.094
Water	197.2	0.197
Fine Aggregate	758.7	0.286
Coarse Aggregate	1135.8	0.422
Sum	2395.2	1.000

Specimens from this concrete were subjected to water permeability tests. The estimated mass proportions of various components of the concrete as tested are given in Table 7.

Table 7

Estimated Mass Proportions of Solids and Free Water in Core (see Appendix A)

		Mass kg/m^3				
Core Reference	Original W/C	Unhydrated Cement	Hydrated Cement	Free Water	Aggregate	Total
3	0.64	62	298	146	1878	2385
4	0.68	53	266	141	1931	2391
5	0.78	40	229	143	1966	2378
9	0.75	55	302	180	1782	2319
11	0.65	57	274	137	1932	2400
Control*	0.65	91	266	157	1895	2409
DOH (9)	0.45	120	315	115	1925	2475

* Fresh concrete designed to simulate the average characteristics of cores 3, 4 and 11 about 28 days after casting.

3. RESULTS

3.1 Water and Gas Permeabilities

The results of tests on individual specimens are given in Appendix B and summarized in Table 8 together with values from other reports (5, 6) for comparison.

3.2 Special Features of Water Permeability

It was noticed as the test proceeded that flow rate decreased with time. It was suspected that this was due to further hydration of the cement during the test; resulting in a weight increase of the specimen. In fact most of the specimens lost weight; in the others it remained constant or showed a small "gain" which was probably due to experimental error. This led to examination of the effluent by mass spectroscopy and by determination of total dissolved solids.

The results of this work are summarized in Figures 11 through 13, and Table 9 and Appendix C.

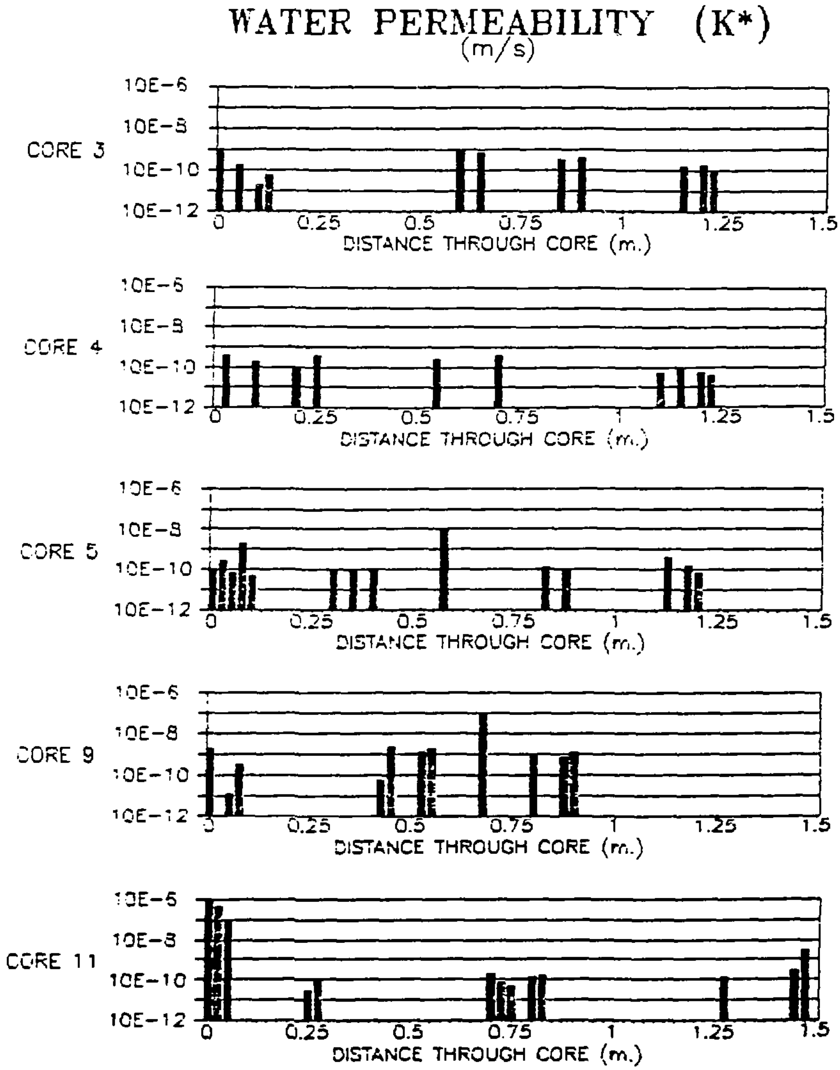

Fig. 11 Variation of apparent permeability with core location and position along its length. The datum for the control concrete is at 2.7 x 10E - 12 m/s, i.e. close to the baseline.

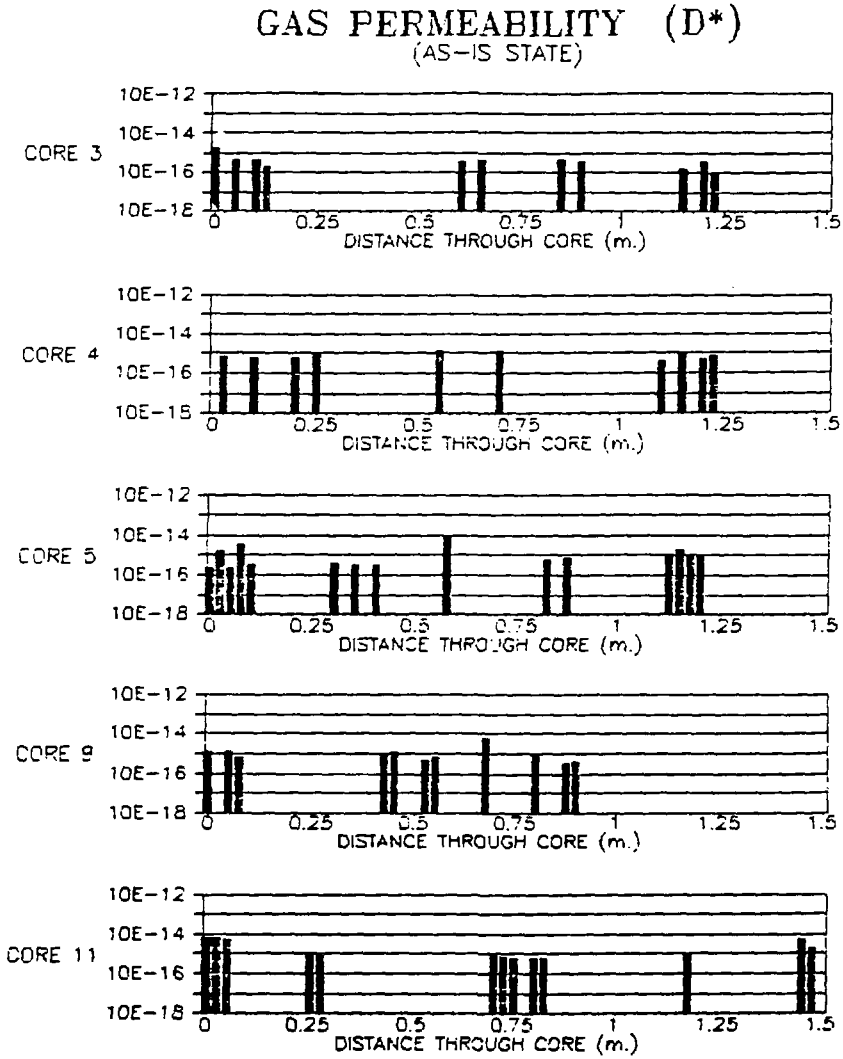

Fig. 12 Gas permeability of partially saturated cores

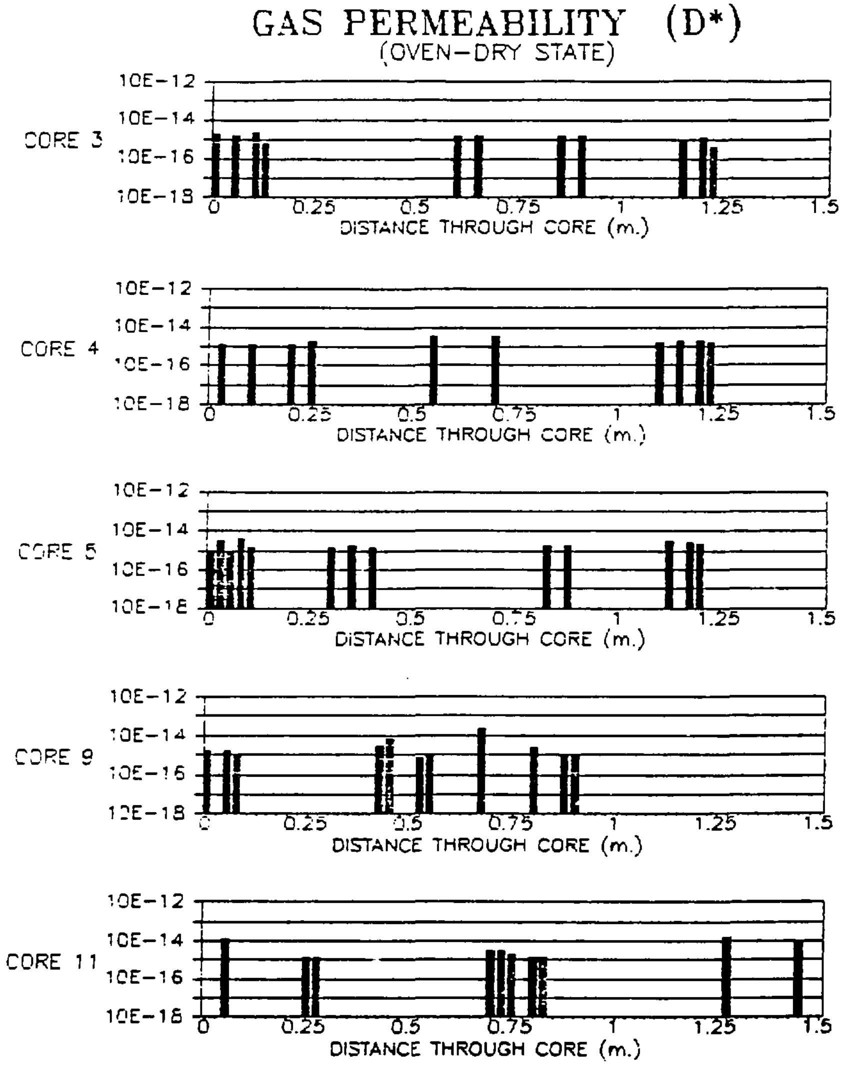

Fig. 13 Gas permeability of oven-dried cores

Table 8

Summary of Permeability Tests and Comparison with Previous Results. Mean values for NPD cores 3 to 11 were averaged over the whole length.

			Water Permeability		Gas Permeability	
Core	No. of Specimens		D* 10 E-18 m^2	k 10 E - 12 m/s	D* As is	10 E - 18 m^2 Oven dry
3	11	$\bar{x}$	33.8*	336	470	1249
		s	28.8	310	429	480
4	10	$\bar{x}$	17.3	182	771	1932
		s	13.2	138	310	856
5	14	$\bar{x}$	93.3	964	1650	2035
		s	25.1	255	2323	928
9	11	$\bar{x}$	34.5	357	783	1697
		s	32.1	331	344	894
11	13	$\bar{x}$	12.8	133	1313	4208
		s	7.5	78	OOR	4734
Control*	15	$\bar{x}$	0.26	2.60	-	-
INFO 011 Table 1		s	0.30	3.10	-	-
INFO 0188		$\bar{x}$	-	39.4	-	-
Table 2	12	$\bar{x}$	3.2	33.5	-	-
		s	4.3	46.1	-	-
INFO 0188		$\bar{x}$	1.9	20.5	-	-
Table 3	12	s	2.2	23.4	-	-
INFO 0111		$\bar{x}$	0.24	2.57	-	-
	6	s	0.10	1.10	-	-
INFO 0188		$\bar{x}$	-	-	-	180
Table 13	7	s	-	-	-	77
INFO 0188		$\bar{x}$	-	-	3.2	-
Table 9	7	s	-	-	2.1	-
DHO 1971		$\bar{x}$	0.039	0.41	59	184
report (9)		s	0.027	0.360	21	57

$\bar{x}$ = mean, s = standard deviation, * this means D* = 33.8 10E-18 m^2

Table 9

Total dissolved solids in effluent

Specimen	Total dissolved solids ppm
Control	385 (OOR)
3	3845 (2142)
4	6132 (3038)
5	4854 (3638)
9	2929 (2359)
11	1860 (OOR)

OOR = out of range

4. DISCUSSION

The observed values of water and gas permeabilities of the NPD concrete exceeded expectations based on published data (1, 2, 3, 4, 5, 6) and early age tests of concrete made with similar mix proportions. Variations with distance from the source of heat and/or radiation were generally masked by random deviations inherent in the nature of concrete and the test procedures. On this account the differences in permeability shown by specimens exposed to high heat and radiation (cores 4 and 5) and those exposed to zero or moderate heat and radiation (cores 3, 9 and 11) are not significant. The trend in the variation of permeability along the length of each core appeared to be significant in cores 3, 4 and 5 and suggested high transparency towards the warm, dry end of the core. Lower values at the cool, damp end are consistent with the idea that pore water at this end was being replenished with ground water. Thus one might expect increased hydration at the coal damp end and migration of dissolved slats towards the hot, dry end. Core 9 showed a contrary trend and core 11 which was exposed equally on all sides showed relatively little variation. However the control concrete, the INFO-188 concrete and the DHO 19 year old concrete (9) which were not exposed to heat and radiation were also impermeable relative to the NPD concrete.

One of the most serious obstacles arose from inappropriate use of the D'Arcy approach to mass transfer. For instance, the D'Arcy formula:

$$\text{Velocity} = \frac{\Delta Q}{\Delta A} = -k\,\frac{\partial p}{\partial x}$$

is not independent of p (3, 5, 6); In other words the absolute value of driving pressure as well as the pressure gradient should be taken into account.

Table 10

Trends in permeability shown by specimens free of visible defects

Core	Temperature	Radiation	Stress	Hot Dry End	Mean Middle	Cool Damp End
3	Moderate	Moderate	High	70	27.8 (22.3)	10
4	High	High	High	30	17.4 (13.2)	3
5	High	High	High	26	13.1 (10.8)	8
9	Low	Low	High	32	34.6 (32.1)	73
11	Moderate	Zero	High	NA	12.9 (7.5)	28

Table 11

Mass transfer through 1000 m^2 of 1 m thick wall under 1 atm over-pressure

	Mass Transfer Unit	Control	Cores 3	4	5	9	11
All Specimens	kg/year	889	$116.5x10^3$	$59.6x10^3$	$321.6x10^3$	$3.212x10^6$	$44.5x10^3$
Specimens without	kg/year	889	$95.8x10^3$	$59.6x10^3$	$45.2x10^3$	$118.9x10^3$	$44.5x10^3$
Visible defects	ratio	1.0	131	67	362	134	50

In the conversion

$$D^* = \frac{\mu}{\rho g} \cdot k \text{ (Appendix E);}$$

The viscosity μ is very sensitive to temperature and, although this may be partially compensated for by careful measurements of temperature it is not possible, by present techniques, to allow for the role of dissolved solids or the consequences of dissolution and precipitation along the drainage path.

In the water permeability tests it was found that the flow rate reduced with time - another characteristic which is not recognized in the D'Arcy formula and which is due to reaction between concrete and permeating water. This phenomenon is illustrated in Fig. 14. The reduction in flow rate is ascribed to a process of dissolution and precipitation as the movement of solute approaches the discharge end. In this report the data was "normalized" by assumption of the flow rate after two hours as an experimental datum. The extrapolation of such values to service conditions in the field is not valid and they should be used solely as a basis for comparison.

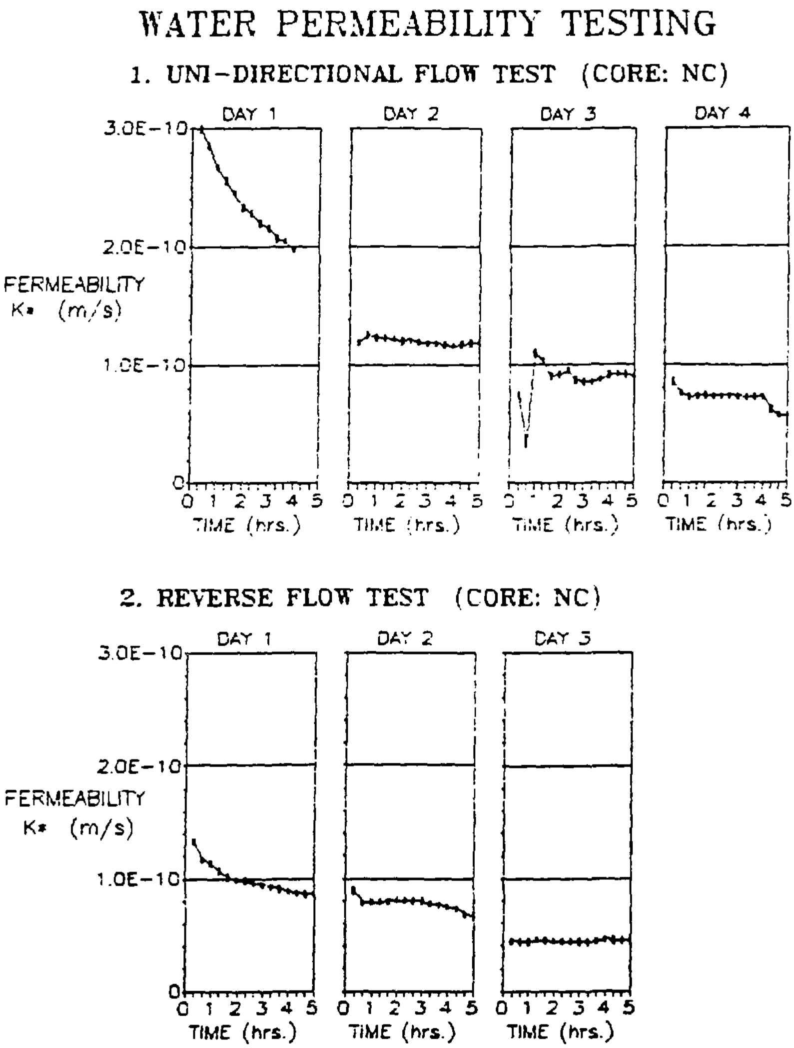

Fig. 14 Reduction of flow rate with time. The first four diagrams are with flow in the direction of coring and the three lower diagrams are for flow in the reverse direction.

5. CONCLUSION

It is well known (7, 8) that the pore structure of concrete changes due to aging. As long as hydration is taking place, the BET surface area, Σ_{BET}, is increasing and the total porosity is decreasing. If the ratio $m = \epsilon/\Sigma_{BET}$ is taken as a function of hydraulic mean radius, it is clear that hydration results in progressive reduction in the size and number of pores capable of transmitting water or gas.

After hydration stops, ϵ remains constant but Σ_{BET} reduces (7) thus m increases and, presumably, so does the capacity of the pore system to transmit a permeant.

In the present work it is clear that the 25 year old NPD concrete is more "transparent" to water and gas than one might have expected at ages of, say, less than 1 year. The extent to which this may be attributed to heat and radiation rather than natural aging is not clear. For instance, referring to Table 10, the difference between core 4, which was exposed to high radiation and temperature, is not significantly different from core 11 which was not exposed to radiation. This should be evaluated by further tests on, say, cores 2, 4 and 11 using larger samples of, say 5 discs for each core.

The phenomenon of reducing flow rate with time calls into question the use of water as a permeant. The observed solubility of alkalis in the permeating water needs further investigation by X-ray and Microscopic analysis.

Setting aside the issues of construction defects and structural cracks, it seems unlikely that the observed increases in permeability were of a magnitude likely to render the concrete unserviceable as a shield for a life of, perhaps, 20 to 30 years. The apparent increase in solubility is nevertheless worrying because of possible long term effects in storage vaults for instance where the required service life is measured in hundreds of years.

6. RECOMMENDATIONS

6.1 This report presents prima facie evidence of increased solubility of alkalis in aging concrete particularly that which was subjected to irradiation and high temperatures. When control tests were done on model concrete, made with modern cement, the effect was not present. This is paradoxical because the modern cement, having been manufactured by the dry process, contains greater quantities of soluble alkalis than cement manufactured 25 years ago. It is recommended that this aspect be further investigated as follows:

(i) SEM and XRD examination to seek evidence of structural degeneration of the hardened cement.

(ii) Repeat tests on 19 year old concrete which was made under carefully controlled conditions being various aggregates and mix proportions under a MTC contract in 1969/71

6.2 Highly radio-active cores from location 2 remain untested because of handling difficulties. It is recommended that these be tested in a protected laboratory by a pressure-decay method which is first calibrated against the results reported herein.

Under the proposed method a small (10 mm) hole is drilled on the axis of the core and a hypodermic needle sealed in place with TRV rubber. The hole is pressurized and then sealed off so that the pressure decay characteristics can be determined. The gas permeability characteristics may then be deduced by a standard procedure (10).

7. REFERENCES

1. Berger, R. University of Illinois, Private Communications, 1989.

2. Mather, B., Callan, E.J., McCoy, E.E. and Carlson, R.W. Permeability and triaxial tests of lean mass concrete. Vicksburg US Army Waterways Experimental Station, Technical Memorandum G-380, March 1954. (see also R.E. Davies, Same title. Berkeley, US Dept. of Army, 128, April 1950).

3. Hooton, R.D. and Wakely. Influence of test conditions on water permeability of concrete in a triaxial cell. Proc MRS Symposium on Pore Structure and Permeability of Cementitious Materials. Boston, October 1988, in press.

4. Hooton, R.D. Permeability and pore structure of cement pastes containing fly ash, slag and silica fume. ASTM STP 987, pp. 128-143, Philadelphia, 1986.

5. Mills, R.H. The permeability of concrete for reactor containment vessels, AECB, INFO-0011, Ottawa, 1983.

6. Mills, R.H. Gas and water permeability of concrete for reactor buildings. AECB, INFO-0188-1 and INFO-0188-2, Ottawa, 1987.

7. Hunt, C.M., Tomes, L.A. and Blaine, R.L. Some effects of ageing on the surface area of cement paste. J. of Res. Nat. Bureau of Standards, Vol. 64A, No. 2, pp. 163-169.

8. Powers, T.C. and Brownyard, T.L. Studies of the physical properties of Portland cement paste, J. Amer. Concrete Institute, Vol. 18, pp. 971-981, April 1947.

9. Mills, R.H. Interfacial Phenomena in Aggregate-Cement Paste Systems. Report to the Department of Highways of Ontario. August 1971.

10. Hsieh, P.A., Tracy, J.V., Neuzil, C.E., Bredehoeft, J.D. and Silliman, S.E. A Transient Method for Determining the Hydraulic Properties of Tight Rock. International Journal of Rock Mechanics Mining Science and Geomechanics, Vol. 18, No. 3, pp. 245-252.

Volume Distribution of Phases in Concrete

The entire quality spectrum of structural concrete is determined by mixing water W between 120 and 240 Kgm^{-3} and water:cement ratio, w_o between 0.28 and 0.75. Taking the density of anhydrous Portland cement = 3220 Kgm^{-3}, we obtain extreme values of cement paste content as follows.

	Mass Kgm^{-3}			Volume lm^{-3}			
Strength (MPa)	w_o	W	C	Water	Cement	Paste	Aggregate
90	0.28	250	857	240	266	506	494
20	0.75	120	160	120	50	170	830

In practice, for concrete in the strength range 30 to 50 MPa, w_o varies between 0.45 and 0.6 and W varies between 160 and 200 Kgm^{-3}, the aggregate volume varies between 660 and 770 lm^{-3}, the paste content between 340 and 230 lm^{-3} and initial porosity between 0.16 and 0.20.

When water reacts chemically with unit mass of Portland cement the amount of combined water is w_n^o = 0.253 and its volume is that of unit mass of Portland cement + 0.2530 mass of water - chemical shrinkage. The chemical shrinkage has been found to be V = 0.2584 x the volume of chemically combined water.

We may compute for completely hydrated cement:

For arbitrary volume		For 1 m^3 of hydrate	
Mass	Volume	Mass Kg	Volume l
1.000	0.3106	2007	623
0.253	0.1876	508	377
1.253	0.4982	2515	1000

In nature, cement is never completely hydrated and the ultimate degree of hydration may be determined [Ref. 22] by the empirical relationship

$$S^* = \frac{1.031\, w_o}{0.194 + w_o}$$

Thus, at ultimate hydration we compute

		Arbitrary Units	
(a)	For unit mass cement	Mass	Units
	Unhydrated cement	$1-S^*$	$\frac{1}{3.22}(1-S^*)$
	Hydrated cement	$1.253S^*$	$\frac{1}{2.515}(1.253S^*)$
	Evaporable water	$w_o + 0.0654S^*$	$w_o + 0.0654S^*$
	TOTALS	$1 + w_o + 0.0654S^*$	$\frac{1}{3.22} + w_o$
(b)	For lm^3 of cement paste	Mass	Volume l
	Unhydrated cement	$\frac{3220(1-S^*)}{1 + 3.22\,w_o}$	$\frac{1000(1-S^*)}{1 + 3.22\,w_o}$
	Hydrated cement	$\frac{4036S^*}{1 + 3.22\,w_o}$	$\frac{1604S^*}{1 + 3.22\,w_o}$
	Evaporable water	$\frac{3220w_o + 604S^*}{1 + 3.22\,w_o}$	$\frac{3220w_o + 604S^*}{1 + 3.22\,w_o}$
	TOTALS	$\frac{3220(1+w_o) + 202S^*}{1 + 3.22\,w_o}$	1000

Considering now 1 m^3 of paste and following Powers [Ref. 20, page 402] we assume the surface area of hydrated cement = 210 m^2g^{-1} and therefore, for lm^3:

$$\text{Surface area} = \frac{210.000\ .\ 403S^*}{1 + 3.22\,w_o}$$

$$= \frac{848 \times 10^6 S^*}{1 + 3.22\,w_o}\ m^{-1}$$

The monolayer capacity, V_m is approximately 0.261 (mass of non-evaporable water) [Ref. 29].

i.e. $V_m \quad \frac{(0.261)(0.253)(3220)S^*}{1 + 3.22\,w_o}$

$(638S^*)/(1 + 3.22w_o)$

The quantity of immobile water 3 V_m [Ref. 20]. This is sometimes called gel water. We define

$$V_{gel} = 3V_m = (1914S^*)/(1 + 3.22w_o)$$

The capillary water = the total evaporable water - the gel water

$$V_{cap} = (3.220w_o - 1310S^*)/(1 + 3.22w_o)$$

Three parameters are used in the Powers and Kozeny-Carman models for permeation through concrete:

$$\text{Void Ratio} \quad N = \frac{V_{gel} + V_{cap}}{1000}$$

$$= (3.220w_o + 0.604S^*)/(1 + 3.22w_o)$$

$$\text{Effective pore space} \quad N_e = V_{cap}/1000$$

$$= (3.22w_o - 1.310S^*)/(1 + 3.22w_o$$

$$\text{Surface area} \quad V = (848E6S^*)/(1 + 3.22w_o)$$

Concrete

For concrete the values of N, N_e and V are adjusted by multiplying the above values for paste by the volume ratio of cement paste in the concrete.

For example, suppose we have concrete with W = 200 Kgm^{-3} and w_o = 0.5.

We compute C = 400 Kgm^{-3}

$$V_c = \frac{400}{3.22} = 124.22 \text{ l}$$

$$W = 200.00 \text{ l}$$

$$\text{TOTAL} = 324.22 \text{ l}$$

The factor is 0.324

Further, $S^* = 0.74$
$N = 0.144$
$N_e = 0.059$
$V = 78 \times 10^{-6} \text{ m}^{-1}$

Sources of error. It is likely that the gel water is highly compressed and, contrary to our assumption, has a specific volume < 1.

Table B1

Results of individual permeability tests

Core	Disks	Distance thru Core (m)	Water Permeability D* (10E-18) (m^2)	Water Permeability K* (10E-12) (m/s)	Gas Permeability D* (10E-18) (m^2) As-Is	Gas Permeability D* (10E-18) (m^2) Oven-dry
3A						
1	3A1/A Surface $\bar{c}$ paint	0.000	93.2	961.7	1701.0	1605.0
2	3A1/B	0.050	18.0	186.1	469.3	1291.0
8	3A6/1	0.60	71.5	737.7	404.8	1398.0
9	3A6/2	0.65	59.5	614.6	459.2	1535.0
5	3A9/1	0.89	29.6	305.8	438.7	1472.0
6	3A9/2	0.90	39.2	404.6	381.5	1401.0
10	3A10/1	1.15	14.6	150.5	173.1	731.2
11	3A10/2	1.20	10.3	106.4	95.8	442.7
3B						
1	3C1/A Surface $\bar{c}$ paint	0.090	4.5	50.59	218.4	562.5
4	3C1/2	0.095	16.0	16.50	480.6	2029.0
7	3C1/M	1.20	'15.4	158.8	342.5*	1266.0

* Retest-Value

Results of individual permeability tests cont'd

Core	Disks	Distance thru Core (m)	Water Permeability D* (10E-18) (m^2)	Water Permeability K* (10E-12) (m/s)	Gas Permeability D* (10E-18) (m^2) As-Is	Gas Permeability D* (10E-18) (m^2) Oven-dry
4A						
6	4A1/A Surface $\bar{c}$ paint	0.56	23.3	270.7	1265.0*	3658.0
7	4A3/2	0.70	35.2	363.6	1288.0*	3314.0
8	4A4/1	1.10	4.9	50.43	376.8*	1433.0
9	4A4/2	1.20	5.4	55.34	449.4*	1740.0
4B						
1	4B1/A Surface $\bar{c}$ paint	0.030	33.0	340.7	716.6	1303.0
4	4B1/B	0.100	15.7	161.9	573.7	1211.0
2	4B1/C	0.2	8.2	85.25	577.3	1277.0
3	4B1/F	0.25	35.3	364.1	922.5	1864.0
5	4B4/1	1.15	9.4	97.17	863.5	1795.0
10	4B4/2	1.22	3.1	32.35	743.3	1722.0

* Retest-Value
- Untested disk

Results of individual permeability tests cont'd

Core	Disks	Distance thru Core (m)	Water Permeability D* (10E-18) (m^2)	Water Permeability K* (10E-12) (m/s)	Gas Permeability D* (10E-18) (m^2) As-Is	Gas Permeability D* (10E-18) (m^2) Oven-dry
5A						
1	5A1/1	0.05	7.7	79.92	2370.0	870.0
6	5A2/A	0.30	8.5	91.49	400.2	1397.0
7	5A2/B	0.40	11.5	119.3	317.4	1763.0
8	5A2/C	0.35	8.6	88.29	311.2	1385.0
9	5A5/1 Holes in Spec	0.40	949.0	9802.0	9289.0	*
10	5A6/1	0.57	12.6	129.5	657.2	1726.0
12	5A6/2	0.87	8.5	87.82	708.9	1731.0
15	5A7/1	1.12	41.2	425.0*	1176.0	2317.0
14	5A7/2	1.17	*	*	1848.0	*
5B						
2	5B1/A	0.020	25.8	266.2	1548.0	3236.0
4	5B1/B Holes	0.075	192.2	1985.0	3756.0	4101.0
3	5B1/1 Surface	0.01	10.9	112.5	212.1	799.8
5	5B1/2	0.075	5.3	54.70	309.9	1337.0
11	5B4/1	1.175	16.2	167.5	1018.0	2719.0
13	5B4/2	1.200	7.5	81.67	828.5	2176.0

* Retest-Value

Results of individual permeability tests cont'd

Core	Disks	Distance thru Core (m)	Water Permeability D* (10E-18) (m^2)	Water Permeability K* (10E-12) (m/s)	Gas Permeability D* (10E-18) (m^2) As-Is	Gas Permeability D* (10E-18) (m^2) Oven-dry
9A						
1	9A1/1 Surface Holes	0.000	155.0	1600.0	1097.0	1480.0
3	9A1/2	0.070	32.4	335.0	966.0	950.0
6	9A3/6 Holes	0.450	110.0	1140.0	432.0	790.0
7	9A3/7	0.550	186.0	1920.0	716.0	1090.0
10	9A4/10	0.875	61.2	631.0	440.0	804.0
11	9A4/11 Holes	0.900	134.7	1140.0	357.0	805.0
9B						
2	9C1/2	0.050	1.2	12.13	1039.0	1450.0
4	9C2/5	0.425	5.5	57.0	1032.0	2680.0
5	9C2/6 Small Cracks	0.450	195.0	2000.0	1137.0	6170.8
8	9C3/9 Holes	0.660	9300.0	96000.0	5950.0	20600.0
9	9C3/11	0.787	72.7	751.0	770.0	2600.0

* Retest-Value

Results of individual permeability tests cont'd

Core	Disks	Distance thru Core (m)	Water Permeability D* (10E-18) (m^2)	Water Permeability K* (10E-12) (m/s)	Gas Permeability D* (10E-18) (m^2) As-Is	Gas Permeability D* (10E-18) (m^2) Oven-dry
11A						
4	11A1/4	0.241	3.0	30.6	850.0	1365.0
11	11A/14	1.270	12.3	127.5	943.0	15000.0
1	11A1/1 Surface large cr	0.000	82200.0	848000.0	6080.0	*
3	11A1/2	0.050	7890.0	81900.0	5730.0	13600.0
5	11A1/5	0.267	11.7	121.0	863.0	1380.0
8	11A3/9	0.750	5.4	56.0	661.0	2150.0
7	11A3/10	0.740	8.0	82.1	687.0	3300.0
11E						
6	11E3/5	0.700	19.3	199.4	984.0	2800.0
9	11E4/7	0.80	13.2	136.3	599.0	1400.0
10	11E4/8	0.825	15.2	156.4	639.8	1380.8
12	11E5/12	1.450	28.0	289.6	5590.0	9095.0
13	11E5/13 Surface bad spec	1.475	29.1	3000.0	2160.0	*
2	11E1/1 Holes crack	2.00	45700.0	472000.0	6642.0	*

* Retest-Value

Table B2

Specimens with visible damage and defects which should be disregardedin Table B1

Core Ref	Specimen with visible defects
3	3A1/A
4	None
5	5A5/1 5B1/B
9	9A1/1 9A3/6 9A3/7 9A4/11 9C2/6 9C3/9
11	11A1/1 11A1/2 11E5/13 11E1/1

Table B3

Permeability tests of Control Specimens

Core	Disks	Water Permeability D* (1 x 10E-18) (m²)	Water Permeability K* (1 x 10E-12) (m/s)	Total Dissolved Solid in Effluent p.p.m
A	1	0.15	1.525	-
	5	0.27	2.837	-
	5*	0.05	0.473	57
N/A	8	0.14	1.489	-
B	3	0.05	0.467	118
	3*	0.05	0.470	-
	9	0.13	1.383	887
	9*	1.39	14.31	-
C	3	0.39	4.068	62
	3*	0.05	0.507	-
	6	0.08	0.825	-
	6*	0.71	7.332	-
D	2	0.09	0.973	745
	2*	1.50	15.58	-
	6	1.00	10.42	438

* Reverse Flow direction

p.p.m. = parts per million

Table B4

Permeability Tests of 19 year old concrete from DHO Contract on Interfacila Phenomena in Aggregate-Cement paste systems 12 August 1975.

Aggregate Specimen	Water Permeability D* (x 1 E - 20 m^2)		Gas Permeability D* (x 1 E - 18 m^2)	
	Initial	Reverse Flow	As Received	Oven Dry
0-1	1.2	1.8	40.0	126.0
0-3	2.4	3.5	68.8	165.7
0-5	4.0	11.4	67.7	208.4
0-7	2.9	6.0	54.0	162.6
0-9	8.0	22.2	120.7	336.7
B-1	2.5	4.9	59.1	183.2
B-3	2.3	9.4	30.5	96.1
B-5	6.0	85.0	47.4	151.7
B-7	3.3	18.0	49.5	192.1
B-9	2.1	11.3	50.3	153.1
B-11	6.0	19.5	66.2	203.8
BL-1	0*	2.3	44.5	137.2
BL-3	5.0	6.1	54.7	223.4
BL-5	1.1	5.5	51.2	164.7
BL-9	7.6	15.9	56.6	174.3
BL-11	9.6	19.6	83.1	270.4

Table C1

Concrete Permeability Tests - Effluent Analysis by Mass Spectroscopy

Sample	Quantity (g)	pH	Cations (mg/l) K+	Na+	Ca++	TS mg/l
3A1-A IT	28.03	12.3	431	681	1.17	2819
3A1-A RFT	28.25	12.3	315	512	0.02	1867
3A1-B IT	13.73	12.7	809	1461	0.03	5070
3A1-B RFT	15.20	12.7	824	1424	3.18	5048
3A6-1	92.74	12.8	562	1420	2.75	4638
3A6-2	84.73	12.7	425	1146	1.50	3515
3A9-1	48.73	12.7	434	1214	1.31	3731
3A9-2	51.93	12.8	477	1311	0.59	4174
3A10-1	48.24	12.3	182	663	0.02	1939
3A10-2	18.47	12.1	107	408	0.10	1143
3C1-A	21.72	12.8	1333	2367	0.25	9723
3C1-2	11.54	12.0	481	1029	0.10	3329
3C1-M	23.32	13.0	968	2098	0.20	3108
4A3-1	44.53	12.8	511	1202	0.35	4655
4A3-2	81.75	12.8	576	1382	0.12	6523
4A4-1	10.94	12.5	579	964	0.17	3937
4A3-2	15.96	12.6	670	1112	0.08	4528
4A1-A IT	30.61	12.9	1433	2026	0.25	10315

TS = Total Solids in Solutions
IT = Initial Test
RFT = Reverse Flow Test

Concrete Permeability Tests - Effluent Analysis by Mass Spectroscopy cont'd

Sample	Quantity (g)	pH	Cations (mg/l) K+	Na+	Ca++	TS mg/l
4B1-A RFT	28.06	12.6	445	498	30.06	3272
4B1-B IT	16.15	12.0	924	1935	1.72	11557
4B1-B RFT	27.88	12.9	1049	1552	1.43	8095
4B1-C	12.44	12.7	746	1419	5.05	6824
4B1-D IT	16.41	12.7	712	1104	2.56	4705
4B2-D RFT	16.51	12.3	209	350	0.54	1594
4B1-D	46.98	12.8	734	1499	5.60	7109
4B4-1	35.55	12.9	960	1994	2.46	10046
4B4-2	9.89	12.4	351	636	0.28	2682
5A1-1	21.14	12.1	217	510	0.19	1654
5A2-A	18.37	12.6	407	958	0.35	2917
5A2-B	16.61	12.7	672	1688	0.23	5553
5A2-C	17.51	13.7	587	1365	0.12	4266
5A2-1	82.33	12.8	25	61	3.60	1634
5A5-1	26.85	12.8	1149	2100	0.25	7359
5A6-1	36.00	12.8	1876	2074	0.18	7303
5A6-2	66.27	12.5	345	582	1.10	2281
5A7-1	19.30	13.8	2036	2610	0.22	14574
5B1-1	69.09	12.8	651	1391	2.54	4514
5B1-A	34.17	12.9	1549	2391	0.17	8699
5B1-B IT	30.58	12.5	346	498	33.97	2124
5B1-B RFT	30.10	12.5	399	588	32.27	251

Concrete Permeability Tests - Effluent Analysis by Mass Spectroscopy cont'd

Sample	Quantity (g)	pH	Cations (mg/l) K+	Na+	Ca++	TS mg/l
5B4-1	36.36	12.6	559	1016	0.19	3588
5B4-2	36.58	12.7	837	1528	0.29	6055
A5	8.08	-	27	55	11.21	57
A8	3.39	-	37	65	8.85	-
B3	8.19	-	28	75	11.03	118
B9	21.94	11.8	107	199	0.07	887
C3	8.06	-	42	75	6.45	62
D2	16.91	11.9	107	161	0.15	745
D6	12.10	-	90	128	0.96	438

Table D1

Water permeability tests on previously tested specimens from cores 9 and 11 and on a fresh sample (NC) of concrete for core 11.

No.	Sample Label	Quantity (g)	pH	Cations (mg/l) K^{+}1	Ca^{2+}	Na^{+}	TS Mg/l
1	9C1-2	26.8	12.6	382	26.0	448.9	1499
2	9C1-2 Ret	14.0	8.5	32	8.22	84.9	1574
3	11A3-11	26.0	12.5	338	11.2	421.7	2701
4	11A3-11 Ret	27.3	12.2	145	40.0	155.2	1020
5	9A4-11	16.1	11.4	61	0.57	129.1	954
6	9A4-11 Ret	25.4	10.6	44	5.44	107.4	750
7	9A1-2	12.5	12.4	516	0.46	1169.	5219
8	9A1-2 Ret	5.1	9.1	67	2.85	-	-
9	9A1-1	25.8	12.5	408	55.0	1251.	6347
10	9A1-1 Ret	13.8	12.3	410	1.00	1346.	6299
11	NC Day 1	27.5	12.7	952	0.03	1289.	7046
12	NC Day 2	27.0	12.7	1112	0.08	1333.	7607
13	NC Day 3	27.0	12.7	987	0.11	1176.	6055
14	NC Day 4	22.0	12.6	831	0.93	1044.	6036
15	NC Day 5	27.0	11.8	399	0.19	407.5	3334
16	NC Day 6	28.0	12.0	401	0.20	389.1	2620
17	NC Day 7	26.6	11.8	389	0.43	375.7	2480

By D'Arcy

$$Q = \frac{k}{\rho g} \cdot A \cdot \frac{\Delta P}{l}$$

and in absolute terms

$$Q = \frac{D^*}{\mu} A \frac{\Delta P}{l}$$

Combining these expressions

$$D^* = k \cdot \frac{\mu}{\rho g}$$

In this report the unit of k is m/s and of D^* is m^2.